HIGHLY RESOLVED LARGE EDDY SIMULATIONS OF A LAMINAR-TURBULENT TRANSITIONAL AIR-HELIUM BUOYANT JET IN A TWO VENTED ENCLOSURE: VALIDATION AGAINST PARTICLE IMAGE VELOCIMETRY EXPERIMENTS

E. SAIKALI[1,2,3] G. BERNARD-MICHEL[1] A. SERGENT[2,4] C. TENAUD[2]

[1]CEA Saclay - DEN/DANS/DM2S/STMF/LIEFT, 91191 Gif-sur-Yvette cedex, France

[2]LIMSI-CNRS (ETCM), Université Paris-Saclay, 91405 Orsay, France

[3]IFD, ED391 SMAER, UPMC Paris 06, Sorbonne Universités, 75006 Paris, France

[4]UFR 919 Ingénierie, UPMC Paris 06, Sorbonne Universités, 75005 Paris, France

International Conference on Hydrogen Safety (ICHS 2017)
September 12, 2017 – Hamburg (Germany)

Hydrogen Safety:
Non-nuclear applications

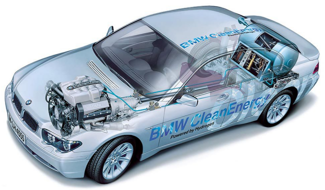

Model: physical set-up

- Fuel cell, garage ⇒ Parallelepiped cavity,
- Hydrogen leakage ⇒ Injection of helium $\rho_{\mathrm{amb}}/\rho_{\mathrm{inj}} = 7.24$ at 25° C (real ratio to hydrogen is 14.38) [Bernard-Michel and Houssin-Agbomson, 2017],
- Reducing the mixture concentration ⇒ Vented cavity,
- Laminar-turbulence transition ⇒ OK [Chen and Rodi, 1980],
- Jet spreading ⇒ OK [Kalter et al., 2014].
- Iso-thermal ans iso-bar conditions: $p = 10^5$ Pa and $T = 298.15$ K.

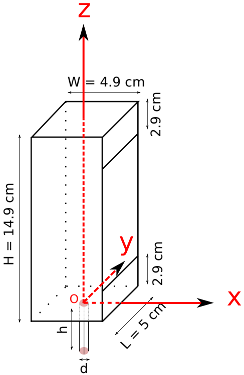

Methodology and key points

Approaches

- Experiment, PIV measurements,
- Numerical approach (currently LES), PIV validation.

Interest

- Buoyant jet regime ($Q = 5$ Nl/min, $\mathrm{Ri}_{\mathrm{inj}} = 0.14$),
- Homogeneous layer with stratification ($\mathrm{Ri}_{\mathrm{v}} = 0.99$),
- Limited domain, two vents, BC issue.

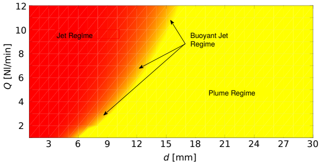

$$\mathrm{Ri}_{\mathrm{inj}} = g \frac{(\rho_{\mathrm{amb}} - \rho_{\mathrm{inj}}) d}{\rho_{\mathrm{inj}} u_{\mathrm{inj}}^2}$$

$$\mathrm{Ri}_{\mathrm{v}} = g \frac{(\rho_{\mathrm{amb}} - \rho_{\mathrm{inj}}) V^{1/3}}{\rho_{\mathrm{inj}} u_{\mathrm{inj}}^2}$$

Main issues

- CFD code challenge (high gradients, rapid laminar-turbulent transition),
- Outlet boundary condition treatment, two outlet challenge,
- Predictive models (free/limited media),
- No similar work reported in the literature.

LES formulation (LMN approximation)

≻ Low Mach Number (LMN) hypothesis ⇒ Pressure = $p(t) + P(\mathbf{x}, t)$ [Müller and Muller, 1999]

$$\begin{cases} \dfrac{\partial \overline{\rho}\widetilde{Y}_1}{\partial t} + \dfrac{\partial}{\partial x_i}(\overline{\rho}\widetilde{u}_i\widetilde{Y}_1) = \dfrac{\partial \overline{\xi}_i}{\partial x_i} + \dfrac{\partial \overline{\xi}_i^{\mathrm{SGS}}}{\partial x_i}, \\ \overline{\rho} = \dfrac{p\overline{M}}{RT}, \\ \dfrac{\partial \overline{\rho}\widetilde{u}_j}{\partial t} + \dfrac{\partial}{\partial x_i}(\overline{\rho}\widetilde{u}_j\widetilde{u}_i) = -\dfrac{\partial \overline{P}}{\partial x_j} + \dfrac{\partial \overline{\tau}_{ij}}{\partial x_i} + \dfrac{\partial \overline{\tau}_{ij}^{\mathrm{SGS}}}{\partial x_i} + \overline{\rho}g_j, \\ \dfrac{\partial \overline{\rho}}{\partial t} + \dfrac{\partial}{\partial x_i}(\overline{\rho}\tilde{u}_i) = 0, \end{cases}$$

where $^{-}$ the spatial filter symbol, $\widetilde{\varphi} = \overline{\rho\varphi}/\overline{\rho}$ (Favre), $\widetilde{\mathbf{u}} = (\widetilde{u}_1, \widetilde{u}_2, \widetilde{u}_3)$, $\overline{\xi}_i = \overline{\rho}\ D\frac{\partial \widetilde{Y}_1}{\partial x_i}$, $D = 6.91 \times 10^{-5}$ $\mathrm{m}^2.\mathrm{s}^{-1}$, $\overline{M} = (\sum_{i=1}^{2} \frac{\tilde{Y}_i}{M_i})^{-1}$, $\overline{\tau}_{ij} = 2\mu\overline{e}_{ij}$ with $\overline{e}_{ij} = \frac{1}{2}(\frac{\partial \tilde{u}_i}{\partial x_j} + \frac{\partial \tilde{u}_j}{\partial x_i}) - \frac{1}{3}\delta_{ij}\frac{\partial \tilde{u}_k}{\partial x_k}$ and $g_j = (0, 0, -g)$.

≻ Additional SGS terms closed as

$$\overline{\tau}_{ij}^{\mathrm{SGS}} = \overline{\rho}(\tilde{u}_i\tilde{u}_j - \widetilde{u_i u_j}) = 2\mu_{\mathrm{SGS}}\overline{e}_{ij} \quad \text{and} \quad \overline{\xi}_i^{\mathrm{SGS}} = \overline{\rho}(\tilde{u}_i\tilde{Y}_1 - \widetilde{u_i Y_1}) = \frac{\mu_{\mathrm{SGS}}}{Sc_{\mathrm{SGS}}}\frac{\partial \tilde{Y}_1}{\partial x_i},$$

where $\mu_{\mathrm{SGS}} = \overline{\rho}(C_s\Delta)^2\sqrt{2\ \overline{e}_{ij}\overline{e}_{ij}}$, $\Delta = (\delta_x\delta_y\delta_z)^{1/3}$, $C_s = 0.18$ and $Sc_{\mathrm{SGS}} = 0.7$ [Blanquart and Pitsch, 2008].

Remark

Average symbols $^{-}$ and $^{\sim}$ are removed for simplicity in the sequel.

Numerical methods & Boundary conditions

- - Semi-implicit scheme (diffusion implicitly), $\mathrm{CFL}_{\mathrm{conv}}$,
  - Finite difference volume on staggered grid,
  - Spatial discretization: 2nd order center (NS-equation), 3rd order QUICK (species) for $Y_1 \in [0, 1]$,
  - Temporal discretization: 2nd order Runge-Kutta,
  - Pressure-velocity incremental projection method (Poisson equation).

- IC's : Cavity filled with pure ambient at rest ($\mathbf{u} = 0,\ Y_1 = 0$),

- BC's : $\partial\Omega = \partial\Omega_w \cup \partial\Omega_i \cup \partial\Omega_o$,
  - *Wall boundaries* ($\partial\Omega_w$). No slip $\mathbf{u} = 0,\ \dfrac{\partial \varphi}{\partial(\mathbf{x} \cdot \mathbf{n})} = 0 \quad : \quad \varphi = \{P, \rho, Y_1\}$.
  - *Injection boundary* ($\partial\Omega_i$). Constant injection mass flux $\rho_{\mathrm{inj}} Q$, Poiseuille $\mathbf{u}$ profile, $\rho = \rho_{\mathrm{inj}},\ Y_1 = 1$.
  - *Outlet boundaries* ($\partial\Omega_o$). Ambient-equilibrium hydrostatic pressure $P = -\rho_{\mathrm{amb}} g z,\ \dfrac{\partial \mathbf{u}}{\partial(\mathbf{x} \cdot \mathbf{n})} = 0$.

    If $\mathbf{u} \cdot \mathbf{n} \geq 0$, then $\dfrac{\partial \varphi}{\partial(\mathbf{x} \cdot \mathbf{n})} = 0 \quad : \quad \varphi = \{\rho, Y_1\}$.
    Else, $Y_1 = 0$ and $\rho = \rho_{\mathrm{amb}}$.

[CEA TRUST-TrioCFD, 2017]

Configuration	Lx [cm]	Cell numbers	MPI procs
0_x		1,134,404	20
1_x	2	2,129,220	40
2_x	3	2,609,476	40
3_x	4.5	3,329,860	60
4_x	6.75	4,427,588	80
5_x	10.125	6,108,484	100

configuration 0_x ***configurations 1_x to 5_x***

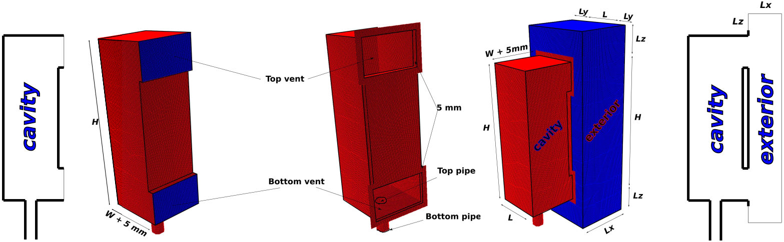

- $\partial\Omega_W$ on red surfaces, $\partial\Omega_i$ on yellow surface and $\partial\Omega_o$ on blue surfaces.
  - Unstructured uniform cubic mesh (per block) with cell size $\delta \approx 7 \times 10^{-4}$ m ($\delta/\eta = 3.3$ [Chhabra et al., 2006] where η denotes the Kolmogorov length scale),
  - 0.5 mm layer around the vents considered as $\partial\Omega_W$ (representing plexi-glass),
  - Pipe $d = 1$ cm, $h = 10$ cm, Poisseuille velocity profile (entrance), $Ly = Lz = 2$ cm .

- physical time of 110 seconds, statistics [70:110] s,
- Velocity magnitude: vertical mid *xz*-plane

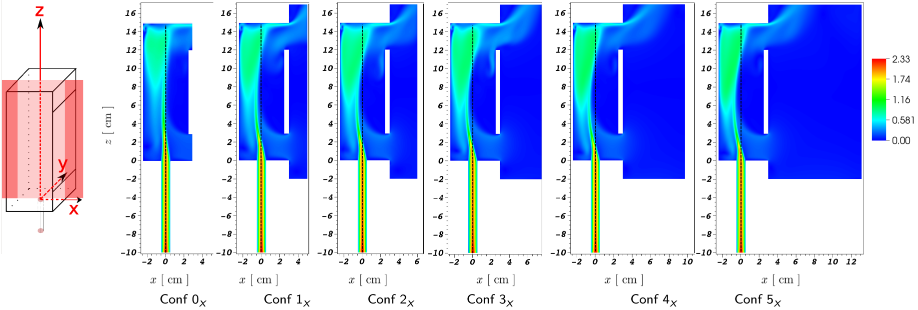

- physical time of 110 seconds, statistics [70:110] s,
- Velocity magnitude: vertical mid xz-plane

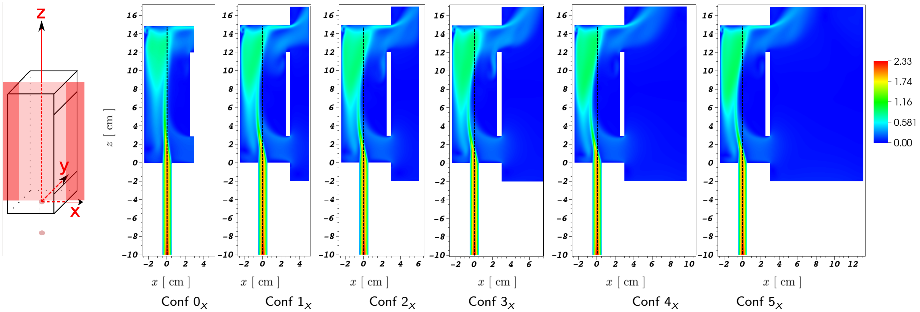

- RMS (velocity magnitude): vertical mid xz-plane

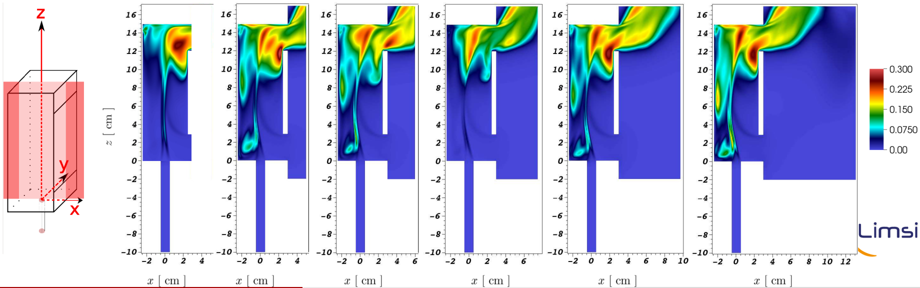

Global quantities and convergence

- Integrated quantities

Configurations	$< \mathcal{M}_{He} >_t$ [$\times 10^{-6}$ kg]	$< Q_v^{bot} >_t$ [$\times 10^{-4}$ $m^3.s^{-1}$]	$< Q_v^{top} >_t$ [$\times 10^{-4}$ $m^3.s^{-1}$]
0_x	8.98677	-2.5817	3.48674
1_x	8.10638	-2.81147	3.71449
2_x	8.30408	-2.80676	3.70839
3_x	8.20663	-2.77233	3.67504
4_x	8.47855	-2.60348	3.49892
5_x	8.45375	-2.60436	3.50027

where $\mathcal{M}_{\text{He}} = \int_{\mathcal{V}} \rho_{\text{He}} X_1 d\mathcal{V}$ denotes the mass of He in the cavity of volume $\mathcal{V}$, $X_1 = \rho Y_1 / \rho_{\text{He}}$ the helium volume fraction. The volumetric flow-rates $Q_v^{\Lambda} = \int_{\partial\Omega_{\text{out}}^{\Lambda}} u_1 d\sigma$, where $\Lambda = \{\text{bot}, \text{top}\}$ and $\partial\Omega_{\text{out}}^{\text{bot}}$, $\partial\Omega_{\text{out}}^{\text{top}}$ denote the surface area of the bottom and top vent respectively.

- L2 norm relative error (conf 5_x is a reference)

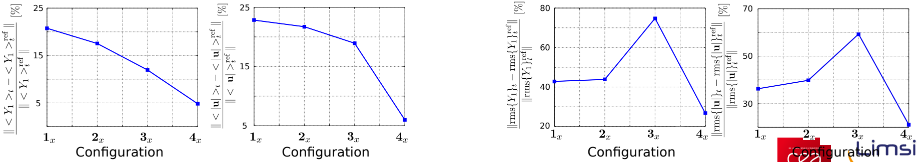

Upper part of the cavity

- Lower cavity flow pattern: vertical mid *xz*-plane,

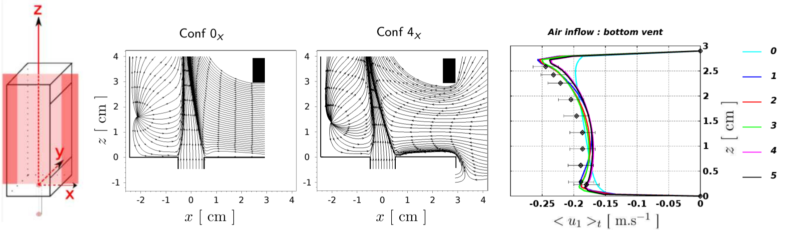

- Lower cavity flow pattern: vertical mid *xz*-plane,

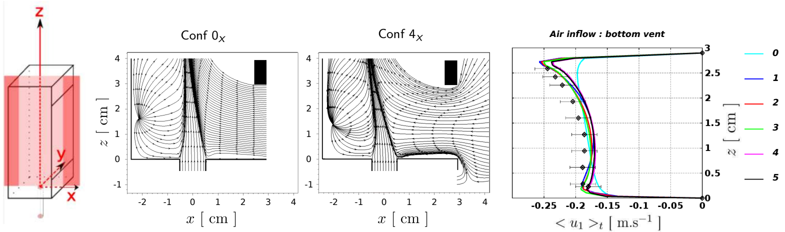

- Vertical *yz*-plane ($x = 2.95$ cm) at the top vent surface : $< u_1 >_t$ *x*-horizontal velocity

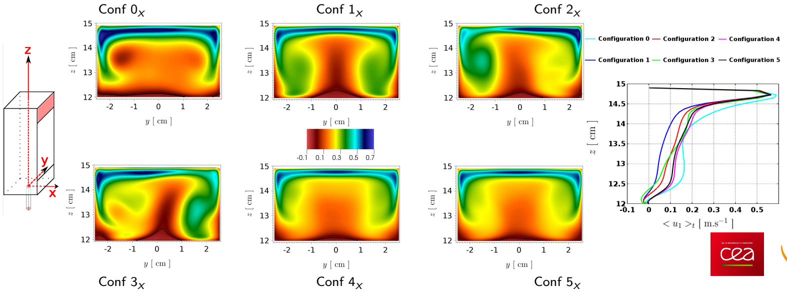

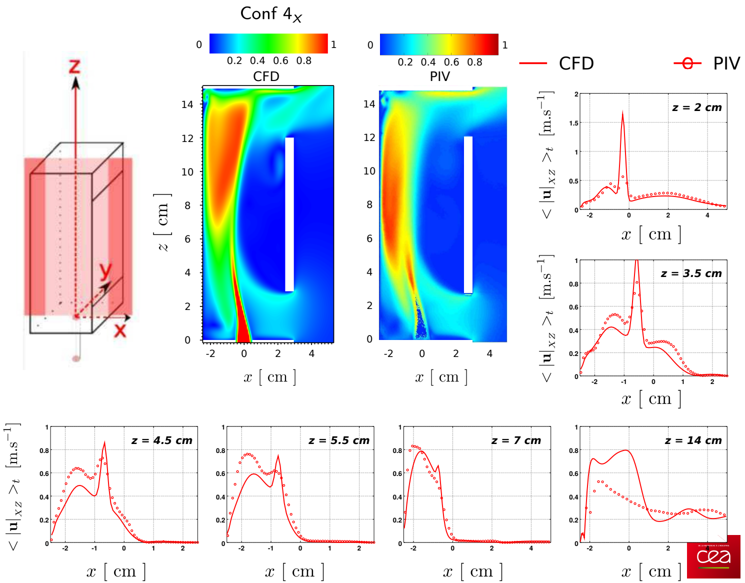
Conf 4_x
CFD
PIV
CFD
PIV
z = 2 cm
z = 3.5 cm
z = 4.5 cm
z = 5.5 cm
z = 7 cm
z = 14 cm
x [cm]
z [cm]
$<|\mathbf{u}|_{xz}>_t$ [m.s^{-1}]

CFD-PIV comparison

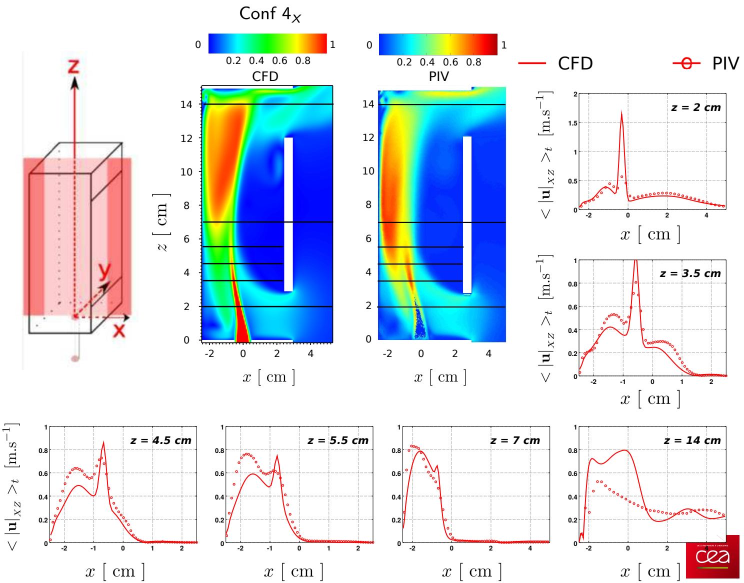

Helium stratification: comparison with Hunt/Linden configuration

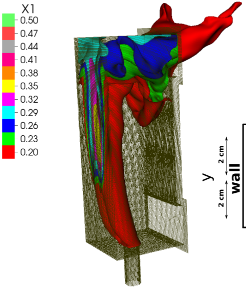

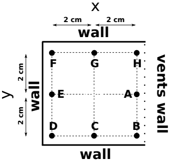

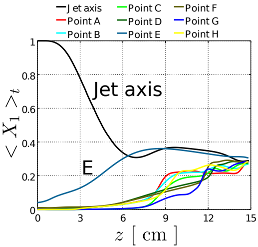

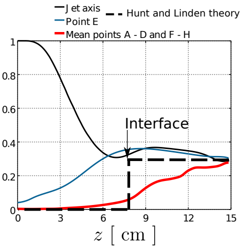

- Two distinct behaviors, small/higher concentrations, E and axis take the highest above $z \approx 6.2$ cm,
- max concentration at top matches well (29 %), thicker layer predicted,
- Geometry dependent, entrainment/mixing process, jet bending effect ...

[Bernard-Michel et al., 2017, Hunt and Linden, 1999, Saikali et al., 2017a]

LES resolution

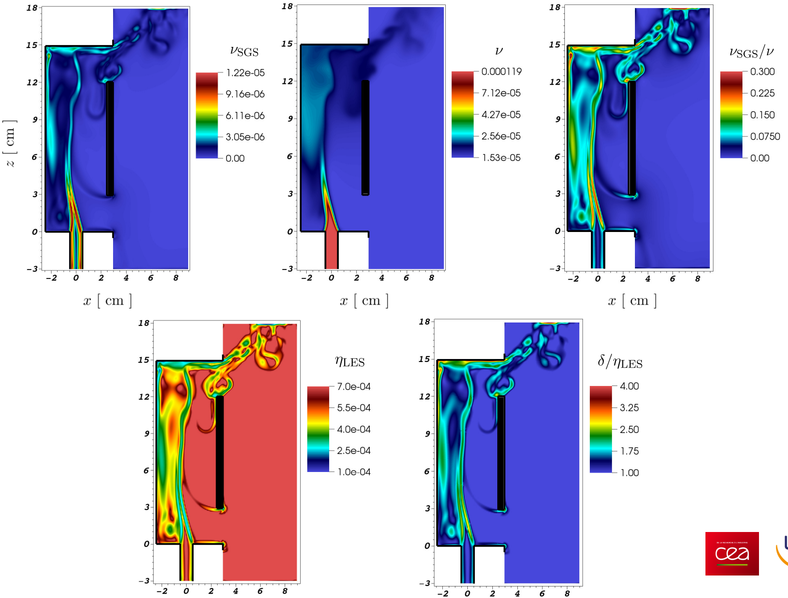

Concluding remarks and discussion

Main conclusion

- Flow analysis: helium distribution, air entrainment, recirculating zones, . . .
- Influence of the outlet boundary condition: similarities and discrepancies,
- Convergence on the size of the exterior domain,
  - Modification of the helium distribution depending the domain size,
  - PIV validation,
- Max concentration predicted by theoretical model, but flow is not divided through a two-layer stratification (Hunt-Linden framework) .

Concluding remarks and discussion

Main conclusion

- Flow analysis: helium distribution, air entrainment, recirculating zones, ...
- Influence of the outlet boundary condition: similarities and discrepancies,
- Convergence on the size of the exterior domain,
  - Modification of the helium distribution depending the domain size,
  - PIV validation,
- Max concentration predicted by theoretical model, but flow is not divided through a two-layer stratification (Hunt-Linden framework) .

Work to be continued (in progress)

- Global validation with new PIV data covering all domain,
- DNS computation ($\eta = 1.75 \times 10^{-4}$ m, $\approx 120 \times 10^{6}$ cells, 1988 MPI procs) for turbulence analysis: from turbulence fluxes and TKE budget to Boussinesq hypothesis validation,

Perspectives

- Development of boundary conditions able to mimic the presence of an exterior domain,
- Increasing the cavity's height and/or increasing/decreasing the injection flow-rate in the objective to produce a two-layer stratification,
- Hydrogen-air cases.

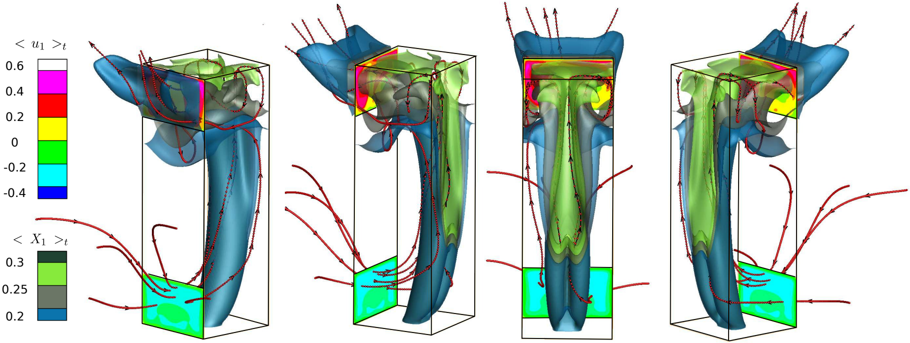

Thanks for your attention !

3D flow description

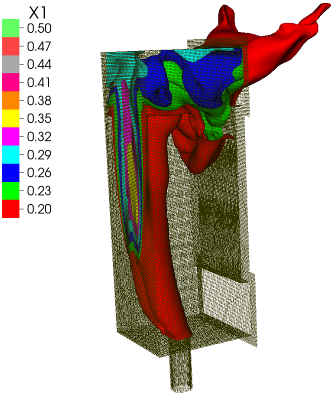

Helium volume fraction

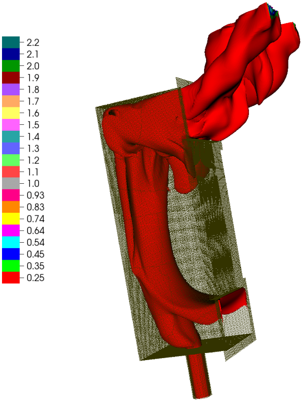

Velocity magnitude

Bibliography I

Bernard-Michel, G. and Houssin-Agbomson, D. (2017).
Comparison of helium and hydrogen releases in 1 m 3 and 2 m 3 two vents enclosures: Concentration measurements at different flow rates and for two diameters of injection nozzle.
International Journal of Hydrogen Energy, 42(11):7542–7550.

Bernard-Michel, G., Saikali, E., and Houssin, D. (2017).
Experimental measurements, cfd simulations and model for a helium release in a two vents enclosure.
In *Proceeding of the International Conference on Hydrogen Safety*.

Blanquart, G. and Pitsch, H. (2008).
Large-eddy simulation of a turbulent buoyant helium plume.
Bulletin of the American Physical Society, 53.

CEA TRUST-TrioCFD (2017).
TRUST-TrioCFD code version 1.7.4.
http://www-trio-u.cea.fr.

Chen, C. J. and Rodi, W. (1980).
Vertical turbulent buoyant jets: a review of experimental data.
NASA STI/Recon Technical Report A, 80.

Chhabra, S., Huq, P., and Prasad, A. K. (2006).
Characteristics of small vortices in a turbulent axisymmetric jet.
Journal of fluids engineering, 128(3):439–445.

Hunt, G. and Linden, P. (1999).
The fluid mechanics of natural ventilation-displacement ventilation by buoyancy-driven flows assisted by wind.
Building and Environment, 34(6):707–720.

Bibliography II

Kalter, R., Tummers, M. J., Bettink, J. B. W., Righolt, B. W., Kenjereš, S., and Kleijn, C. R. (2014).
Aspect ratio effects on fluid flow fluctuations in rectangular cavities.
Metallurgical and Materials Transactions B, 45(6):2186–2193.

Müller, B. and Muller, B. (1999).
Low mach number asymptotics of the navier-stokes equations and numerical implications.

Saikali, E., Bernard-Michel, G., Sergent, A., Tenaud, C., and Salem, R. (2017a).
Highly resolve large eddy simulations of a transitional air-helium buoyant jet in a two vented enclosure: validation against particle image velocimetry experiments.
In *Proceeding of the International Conference on Hydrogen Safety*.

Saikali, E., Sergent, A., Bernard-Michel, G., and Tenaud, C. (2017b).
Large eddy simulations of an air-helium buoyant jet in a two vented enclosure: influence of the outlet boundary condition.
In *Proceeding of the 23ème Congrès Français de Mécanique*.

- 110 seconds of physical time,
- time evolution of the velocity magnitude at a point in the middle of top vent,

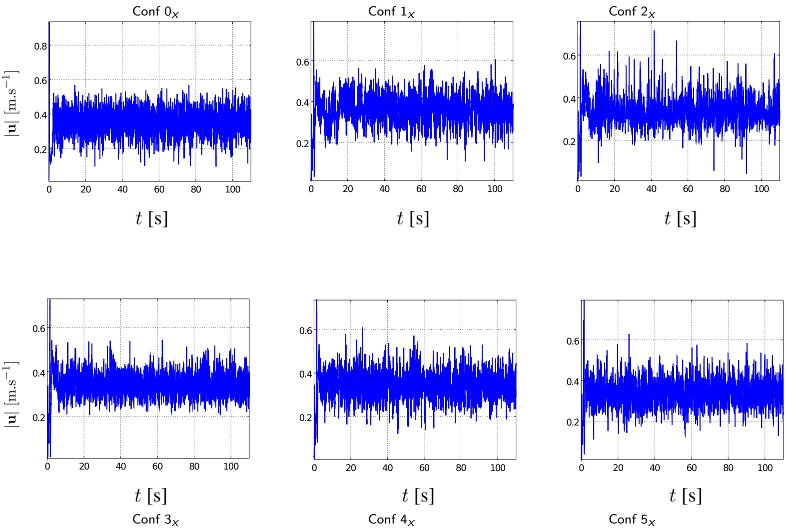

- quasi steady solution asumed to be reached at 70 seconds.